Investigation of a PV Fed Improved Smart Home EV Battery Charging System using Multi Output Hybrid Converter

Arindam Mukherjee*, Krithiga S.**‡, Partha Sarathi Subudhi***

*School of Electrical Engineering, Vellore Institute of Technology (VIT), Chennai, Tamil Nadu 600127, India

**School of Electrical Engineering, Vellore Institute of Technology (VIT), Chennai, Tamil Nadu 600127, India

***School of Electrical Engineering, Vellore Institute of Technology (VIT), Chennai, Tamil Nadu 600127, India

(mukherjee.arindam8@gmail.com, s_krithiga@yahoo.com, partharesearch.vit@gmail.com)

‡Corresponding Author; Krithiga S., School of Electrical Engineering, Vellore Institute of Technology (VIT), Chennai, Tamil Nadu 600127, India, s_krithiga@yahoo.com

Received: 04.02.2019 Accepted:12.03.2019

Abstract- Power converters used in the existing smart home electric vehicle (EV) battery charging systems are capable of feeding only dc power. Whereas, this paper proposes the usage of hybrid converters in such systems as they are used for supplying power to both ac and dc loads simultaneously. Among various hybrid converter topologies, boost derived hybrid converter (BDHC) and quadratic boost derived hybrid converter (QBDHC) are analysed in this paper. A photovoltaic (PV) array fed smart home system using BDHC and QBDHC is proposed to provide both dc power and ac power simultaneously and their performances were compared in this paper. The interfacing of multiple outputs is accomplished using time division multiplexing of power generated from PV array. In the proposed system, the hybrid converter is designed by replacing single switch of conventional boost converter by voltage source inverter (VSI). It has higher reliability in terms of power density and has inherent shoot-through protection during inverter operation. It is best suited for home applications which require support for both ac and dc loads. The system is designed, modelled and simulated using PSIM software and a laboratory prototype is developed and tested. Resemblance between the simulated and experimental results validates the efficaciousness of the proposed system.

Keywords Smart home, Photovoltaic Array, Electric Vehicle Battery, Hybrid Converter.

1. Introduction

Present scenario depicts energy crisis due to fast depleting fossil fuels and environmental issues, which are the consequences of toxins released due to over use of such fuels [1]. Depletion of conventional resources has perpetuated the need for developing non-conventional or renewable energy based systems [2-3]. Renewable energies include solar, wind, hydel, ocean thermal energies, among which solar and wind are most commonly used [4-5]. Utilization of these energies requires power electronic converter, which can control the flow of harnessed energy and suit various applications [6-7].

These power electronic converters include DC-DC converters, inverters, rectifiers and cyclo-converters [8]. Recently, development of hybrid derived converter has further contributed to the advancement of power electronics [9–10]. All these converters are controlled using switches, which was SCRs in earlier days. Now-a-days, modern switches as MOSFETs and IGBTs are used and can operate in wide range of frequency [11-12]. There are various advantages of power electronics over linear electronics such as the efficiency of power electronic devices ranging from 70 to 90 % irrespective of the input voltage [13-14]. The switches operate at their most efficient points of active, saturation and cut-off regions which enable them to deliver higher power to the load [15]. The frequency of operation can be of higher order which reduces the size and cost of passive elements like inductors and capacitors [16].

Nowadays, nano grid architecture is a booming research area which involves small scale energy generation, capable of handling the energy need for a single building or household [17]. Integrating suitable power converters to the

photovoltaic (PV) array can be used to achieve this goal [18-19]. Every house with such system can produce their own energy and can also inject excess power to the grid [20-21]. Thus, energy demand can be reduced by following such architecture.

There are different topologies of hybrid converter [22], one among them is boost derived hybrid converter (BDHC) which can simultaneously supply dc as well as ac power. BDHC is realized by replacing the control switch of a conventional boost converter by H-bridge inverter. The resulting topology has lesser number of switches compared to conventional boost converter cascaded to the inverter. Thus, it finds application in the household as well as in industries and solar power from PV arrays can also be used for pumping power to load or utility grid using such converters.

Recent advances in transportation research focuses mainly on electric vehicle (EV) due to its various advantages over conventional internal combustion engine vehicles [23-25]. In order to charge an EV battery, power electronic interfacing systems are used to feed power from utility grid or renewable energy sources [26-27]. These power electronic interfacing system is also called as EV charger. If the power electronic interfacing system is placed inside the EV, then the charger is called as ON board charger whereas in the OFF board charger, the interfacing system is placed in the charging station [28]. In case of ON board charger, placement of power electronic interface system inside the vehicle results in increase in weight of the EV and reduction in the efficiency of the system which concludes that the OFF board EV battery chargers are preferable over ON board EV battery chargers [29]. Therefore, OFF board EV battery chargers are considered in this system. The proposed smart home system employs BDHC and QBDHC as the power electronic interfaces used in an OFF board EV battery charger.

In this paper, PV fed smart home system is proposed, which employ multi output hybrid converter for feeding power to EV battery as well as ac load or grid simultaneously. The employed hybrid converter adopts single step conversion process for generating dc as well as ac power at the output terminals from the input dc power. The contributions of the paper are listed as follows:

- The paper contributes a novel PV fed smart home system which employ hybrid dual output converter for charging EV battery and feeding an ac load simultaneously. A digital controller is employed in this proposed system for operating the switches of the hybrid converter.
- The proposed system employs lesser number of components compared to the existing smart home systems.
- Single step power conversion process is adopted in this proposed smart home system in order to increase overall system efficiency compared to the existing systems.

The article is outlined into six sections. Section 2 contains description of the proposed system followed by design of the system which is provided in section 3. Section 4 of this article contains simulation studies and results of this multi output hybrid converter system. Hardware investigation of the proposed system is provided in section 5. Section 6 contains the conclusion of the PV fed improved smart home system.

2. Description of the Proposed System

Block diagram of the proposed system is shown in Fig.1. This system consists of a PV module, multi output hybrid converter, ac load and EV battery. In this system, boost derived hybrid converter (BDHC) and quadratic boost derived hybrid converter (QBDHC) have been used as multi output hybrid converter. Power from PV module can be fed to both ac load and EV battery simultaneously. The output voltage is regulated by a controller, which generates gate pulses for the switches in the converter.

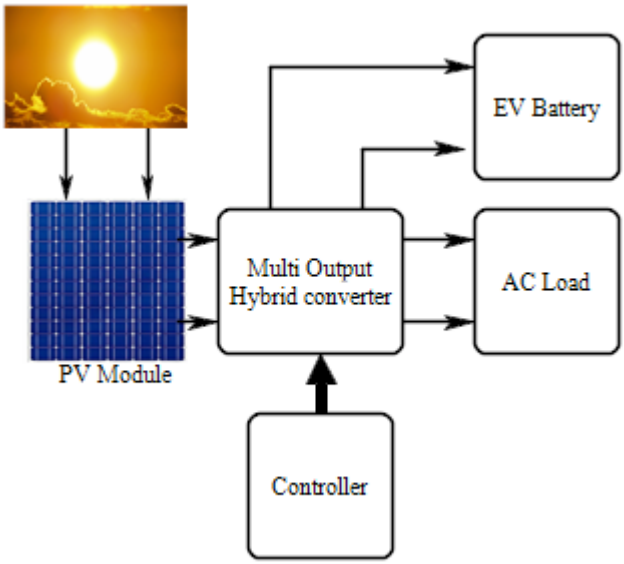

Fig. 1. Block diagram of the proposed multi-output system.

2.1 Operation of the boost derived hybrid converter

In order to generate both dc and ac output simultaneously, the converter operates in three intervals. The intervals are shoot through interval, power interval and zero interval. Details regarding the converter operation during these three intervals are explained in the following subsections.

2.1.1. Shoot through interval

The equivalent circuit of BDHC during shoot through interval is shown in Fig.2. The switches, S_1 & S_4 or S_2 & S_3 are switched ON during this interval. When switches, S_1 & S_4 are ON, current flows through the path PV Module- L_{in}-S_1-S_4-PV Module charging the inductor L_{in}. Also, H-bridge current circulates through S_1-ac load- antiparallel diode of S_3 – S_1. When switches S_2 & S_3 are ON, current flows through the path PV Module- L_{in}-S_3-S_2- PV module. H-Bridge current circulates through S_2-antiparallel diode of S_4-ac load-S_2. The diode, D_1 is reverse biased and the output capacitor, C_{dc} discharges through the EV battery during this interval. The duration of this interval depends on the shoot through duty ratio (D_{st}) of the gate pulses of the converter.

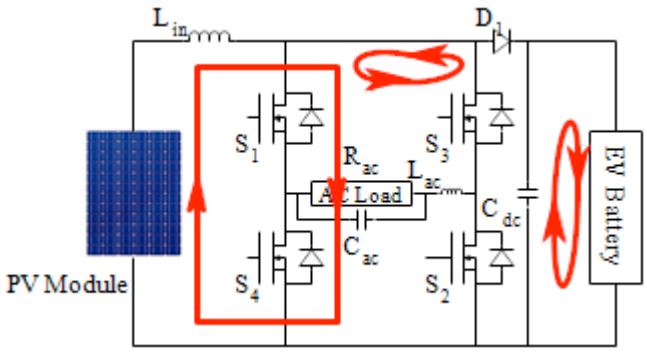

Fig. 2. Operation of the converter during shoot through interval.

2.1.2. Power interval

Circuit operation of BDHC during power interval is shown in Fig.3. Switches, S_1 & S_2 or S_3 & S_4 are in ON state during this interval. Diode, D_1 is forward biased and thus output dc current flows through this diode. During this interval, PV module current flows through inductor, L_{in} and diode, D_1 to charge the EV battery. Also, H-bridge current flows through the switches, S_1 & S_2 to supply ac load from PV module. When switches, S_3 and S_4 are ON instead of switches, S_1 and S_2, PV module current flows through the path, S_3 – ac load- S_4. Inductor discharges through ac load and dc load in this interval. The H-bridge switching is determined by the modulation index, M_a.

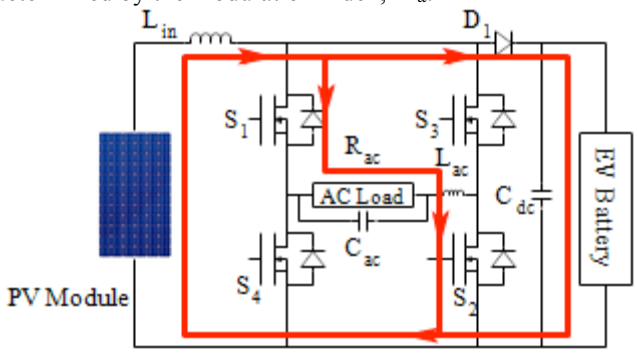

Fig. 3. Operation of the converter during power interval.

2.1.3. Zero interval

BDHC operation during zero interval is shown in Fig.4. In this interval, either upper pair of switches or lower pair of switches i.e. either S_1 & S_3 or S_4 & S_2 are in ON state and the diode D_1 keeps conducting and inverter current circulates through the bridge but is not sunk or sourced. PV module current flows through the path PV Module-L_{in}-D_1-EV battery-PV module.

The operation of QBDHC is similar to the above explained operation of BDHC which is explained in literature [9].

3. Design of the Proposed Multi Output System

The converter used in this system produces dual output (both dc and ac) from a single dc input source. Schematic diagram of the system is shown in Fig.2. In Fig.5a, BDHC 1 is shown which consists of a single inductor, Lac and capacitor, C_{ac} for filtering the ac output voltage. In BDHC 2 shown in Fig.5b, the filter inductor is divided into two parts, L_{ac1} and L_{ac2} which reduces the bulkiness of the inductor. Schematic diagram of the QBDHC is shown in Fig.5c and the operations of the BDHC 1, BDHC 2 & QBDHC are described in literature [9]. Among the above three structures, QBDHC inherits the advantages of the quadratic boost converter to the hybrid converter. This converter is designed in such a way to reduce the ripples in current and voltage waveforms as per IEEE standard 519-1992 [30]. Design equations of BDHC and QBDHC are furnished in the following sections.

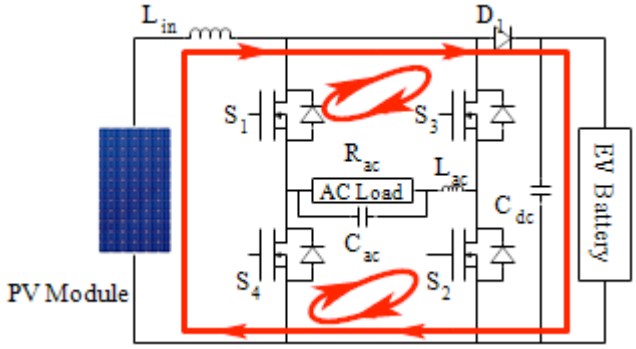

Fig. 4. Operation of the converter during zero interval.

3.1 Design Equations of Boost derived Hybrid Converter

In this section, the necessary equations for designing the BDHC are provided [9].

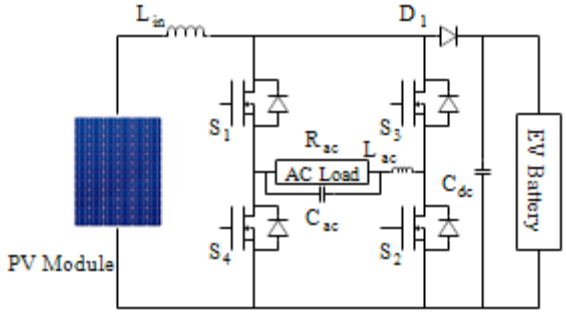

(a)

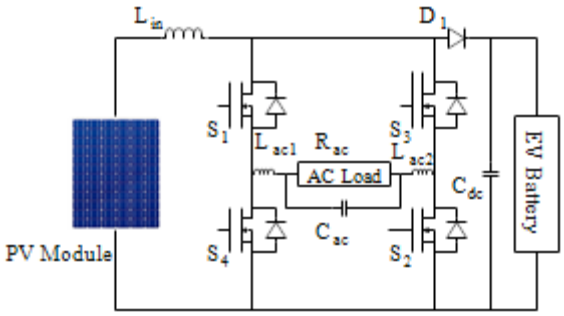

(b)

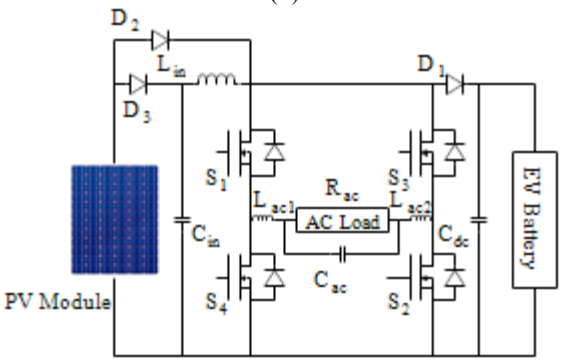

(c)

Fig. 5. Schematic diagram of the proposed system with different structures (a) BDHC 1, (b) BDHC 2 and (c) QBDHC.

The DC voltage gain expression of BDHC is similar to that of a conventional boost converter and is given by:

$$\frac{V_{bat}}{V_{pv}} = \frac{1}{1-D_{st}} \quad (1)$$

Where, V_{bat} is battery voltage, V_{pv} is PV module voltage, D_{st} is Shoot-through duty ratio.

AC voltage gain of the BDHC is as follows:

$$\frac{V_{0ac}}{V_{pv}} = \frac{M_a}{1-D_{st}} \quad (2)$$

Where, V_{0ac} is ac output voltage, M_a is Modulation index. The switching constraint of BDHC is provided by the following equation.

$$M_a + D_{st} \le 1 \quad (3)$$

Output power of BDHC is related to input voltage by equation (4) and (5).

$$P_{bat} = \frac{V_{pv}^2}{R_{bat} * (1-D_{st})^2} \quad (4)$$

$$P_{ac} = \frac{0.5 * M_a^2 * V_{pv}^2}{R_{ac} * (1-D_{st})^2} \quad (5)$$

Where, P_{bat} is battery power, P_{ac} is ac power, R_{bat} is battery internal resistance, R_{ac} is resistance of the ac load. Passive elements of BDHC are designed as follows:

$$L_{in} = \frac{V_{pv} * D_{st}}{f_s * \Delta I} \quad (6)$$

$$C_{dc} = \frac{I_{out} * D_{st}}{f_s * \Delta V} \quad (7)$$

$$f = \frac{1}{2\pi\sqrt{L_{ac}C_{ac}}} \quad (8)$$

Where, L_{in} is input inductor, C_{dc} is DC output filter capacitor. f_s is switching frequency, ΔI is the ripple current of Input inductor, L_{in}, ΔV is capacitor, C_{dc} ripple voltage, I_{out} is maximum dc output current, f is harmonic frequency, L_{ac} is ac filter inductor, C_{ac} is ac filter capacitor.

3.2 Design Equations of Quadratic Boost derived Hybrid Converter

The expressions for dc voltage gain, ac voltage gain, dc power and ac power of a QBDHC are provided in this section. Relation between the dc output voltage (EV battery voltage), V_{bat} and PV module voltage, V_{pv} are given as follows:

$$\frac{V_{bat}}{V_{pv}} = \frac{1}{(1-D_{st})^2} \quad (9)$$

AC output voltage, V_{0ac} and PV module voltage, V_{pv} are related as per equation (10).

$$\frac{V_{0ac}}{V_{pv}} = \frac{M_a}{(1-D_{st})^2} \quad (10)$$

EV battery power, P_{bat} can be expressed as follows:

$$P_{bat} = \frac{V_{pv}^2}{R_{bat} * (1-D_{st})^4} \quad (11)$$

AC output power of the proposed system is given by:

$$P_{ac} = \frac{0.5 * M_a^2 * V_{pv}^2}{R_{ac} * (1-D_{st})^4} \quad (12)$$

Using the design equations 1-12, the proposed system with BDHC and QBDHC are designed and simulated using PSIM simulation software. Simulation studies of the proposed system and its results are presented in the following section.

4. Simulation Studies and Results

BDHC model is developed using the power electronic components and passive elements present in PSIM software. The developed BDHC model is integrated with PV module model and battery model available in PSIM to develop the proposed system as shown in Fig.6. Parameters used for design of BDHC and QBDHC are given in Table 1. The simulation of the proposed system was carried out with both BDHC and QBDHC separately and the results are furnished in this section.

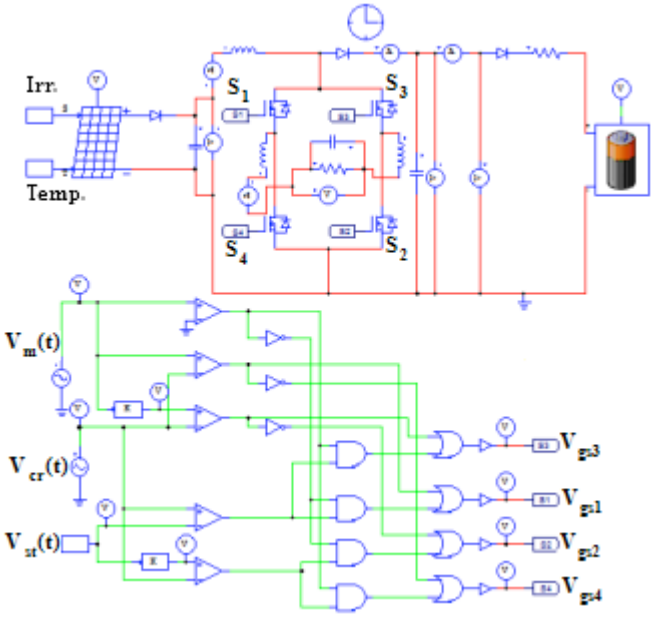

Fig. 6. Simulation model of the proposed system.

Table 1. Parameters used for design of BDHC & QBDHC.

Sl. No.	Parameters	Specifications	
		BDHC	QBDHC
1.	Input Inductor, L_{in}	2 mH	2.5 mH
2.	Output Capacitor, C_{dc}	1200 µF	1200 µF
3.	AC filter inductor, L_{ac}	5.6 mH	5.6 mH
4.	AC filter capacitor, C_{ac}	72 µF	72 µF
5.	Duty Ratio	0.6	0.36
6.	Modulation index	0.4	0.64
7.	Switching Frequency	5 kHz	5 kHz

The gate pulses to the MOSFETs in the converter are provided through a controller which follows unipolar sine pulse width modulation technique with shoot-through duty ratio [31]. The sine wave is compared with a carrier wave, which determines the modulation index, and a constant DC voltage is used to generate shoot-through pulse by comparing it with the same carrier signal. Figure 7 shows the logic diagram of the controller which generates pulses to the converter.

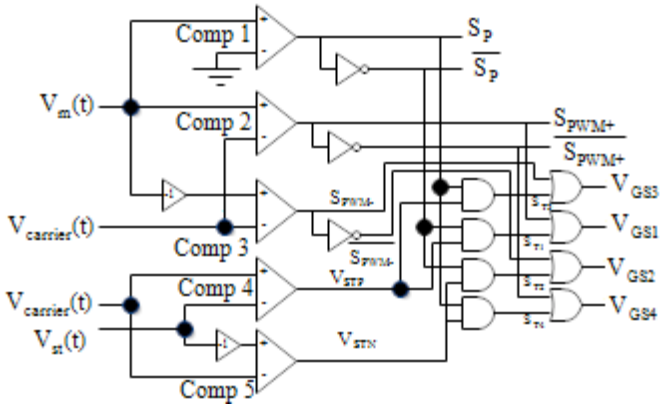

Fig. 7. Logic model of the controller.

The controller consists of five comparators among which the first comparator, comp1 acts as a zero crossing detector (ZCD) comparing a sine wave, $V_m(t)$ with the ground. The next comparators, comp2 and comp3 compares sine wave and 180^0 phase shifted sine wave with the carrier signal, $V_{carrier}(t)$ respectively to produce S_{PWM+} and S_{PWM-} signals. Comparators, comp4 and comp5 compare positive and negative DC voltage, V_{st} with the carrier signal and generate shoot-through pulses. Shoot-through duty ratio is determined by V_{st}. Carrier signal is compared to positive V_{st} in order to generate the signal, V_{STP}. Further, signal V_{STP} is ANDed with ZCD output, $\overline{S}_p$ to get the shoot through pulse, S_{T1} as shown in Fig.7. Thus, to get the final pulse, V_{GS1} for switch 1, S_{T1} is ORed with S_{PWM+}. The resulting pulse has sine wave modulation as well as shoot-through. Similarly, pulse to switch S_4, V_{GS4} is generated by ANDing signal, V_{STN} and S_P and the resulting shoot through pulse S_{T4} is ORed with for a generation of pulses to switches, S_3 and S_2, same technique is followed and the overall PWM scheme is shown in Fig. 5.

In Fig.8, ST, PW and Z represent shoot-through, Power and Zero intervals of gate pulses respectively. It is evident from the figure, that during shoot-through either S_1 & S_4 or S_2 & S_3 are conducting and during Zero interval, either S_1 & S_3 or S_2 & S_4 are conducting and during power interval, S_1 & S_2 or S_3 & S_4 are conducting. This generated PWM scheme is in accordance with the principle of the converter. This controller is used in simulation model of BDHC as shown in Fig.6.

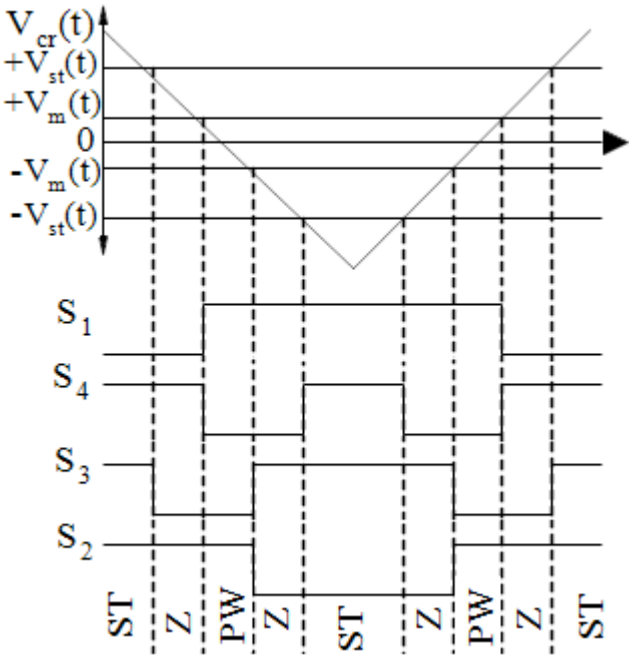

Fig. 8. PWM scheme with intervals.

PV module available in PSIM library is used for simulation study of the proposed system. Power rating of the PV module is considered as 250 W at standard test condition. At an irradiation of 850 W/m^2, PV module voltage and current was observed as 24 V and 8.3 A respectively. The converter was operated at switching frequency of 5 kHz with modulation index and shoot through duty ratio of 0.4 and 0.6 respectively. Waveforms of gate pulses V_{GS1}, V_{GS2}, V_{GS3} and V_{GS4} are shown in Fig.9.

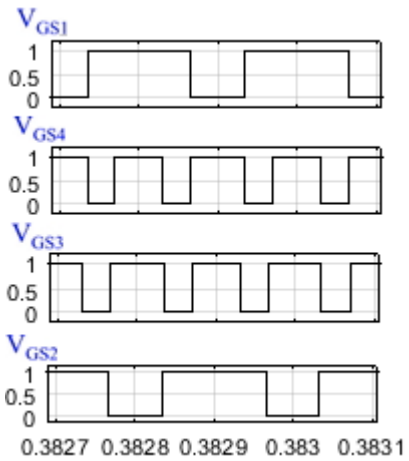

Fig. 9. Gate pulses for the converter.

PV module voltage, V_{pv} and current, I_{pv}, dc output voltage, V_{dc} and current, I_{dc} output ac voltage, V_{0ac} and current, I_{0ac} waveforms are presented in Fig.10. It was found from the simulation results that the dc output voltage and current is 61.5 V and 1.7 A respectively while ac output voltage and current are 16.54 V and 5.53 A respectively. Out of the generated PV power of around 200 W, 105 W is fed to the battery and 92 W is fed to the ac load, contributing to overall system efficiency of 98.5 %. The PV voltage of 24 V is boosted to a dc output terminal voltage of 61.5 V which is sufficient to charge the EV battery. Voltage and current waveforms of the EV battery during charging condition are shown in Fig.11.

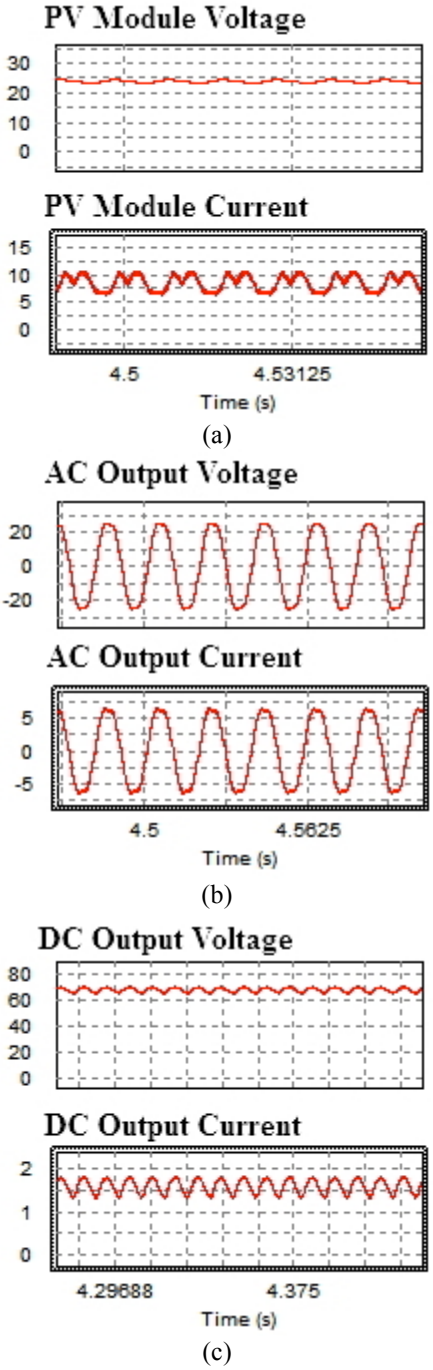

Fig. 10. Voltage and Current waveforms of (a) PV module (b) dc output and (c) ac load of BDHC.

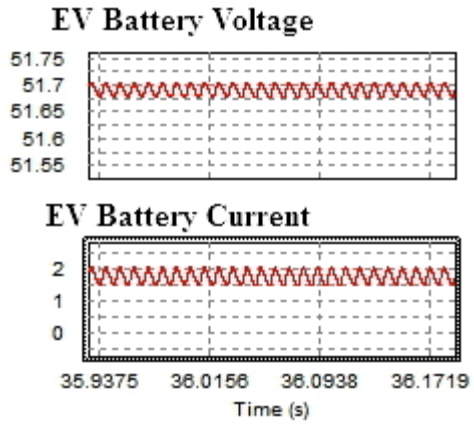

Fig. 11. Battery terminals waveform.

The simulation model of proposed system using QBDHC is shown in Fig.12. At an irradiation of 850 W/m^2, PV module voltage is boosted from 24 V to 60.6 V dc, using a lower Shoot-through ratio of 0.36 and with a modulation index of 0.64 to charge EV battery. At the same time, approximately 99 W power is supplied to ac load with an ac voltage of 24.35 V.

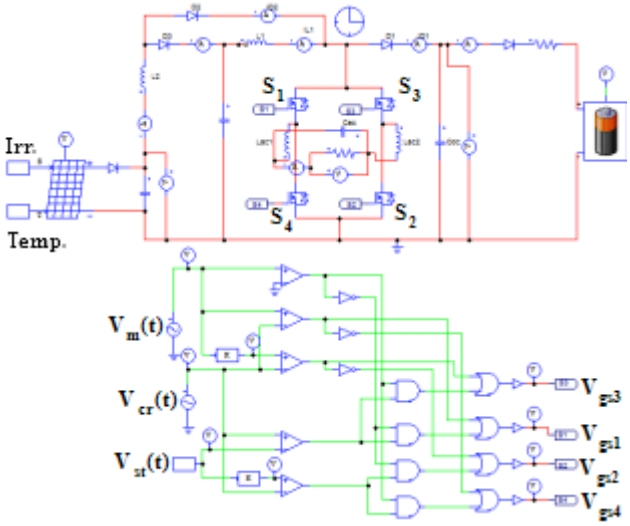

Fig. 12. Simulation model of QBDHC.

Waveform of PV module voltage of 24 V & PV module current of 8.52 A, dc output voltage of 60.59 V & dc output current of 1.68 A and ac output voltage of 24.35 V & current of 4.06 A are shown in Fig.13, which was obtained from the simulation studies.

Out of the PV generated power of 204 W, approximately 103 W is fed to the EV battery and 99 W is fed to the ac load, contributing to overall system efficiency of 98.6 %. From the simulation studies, it is inferred that, for the same power rating, the system with QBDHC is capable of doubling the ac voltage gain with increased efficiency at a lower duty ratio when compared to the system with BDHC.

In order to validate the simulation results, a laboratory prototype is fabricated and tested. Experimental investigation of the proposed prototype is presented in the following section.

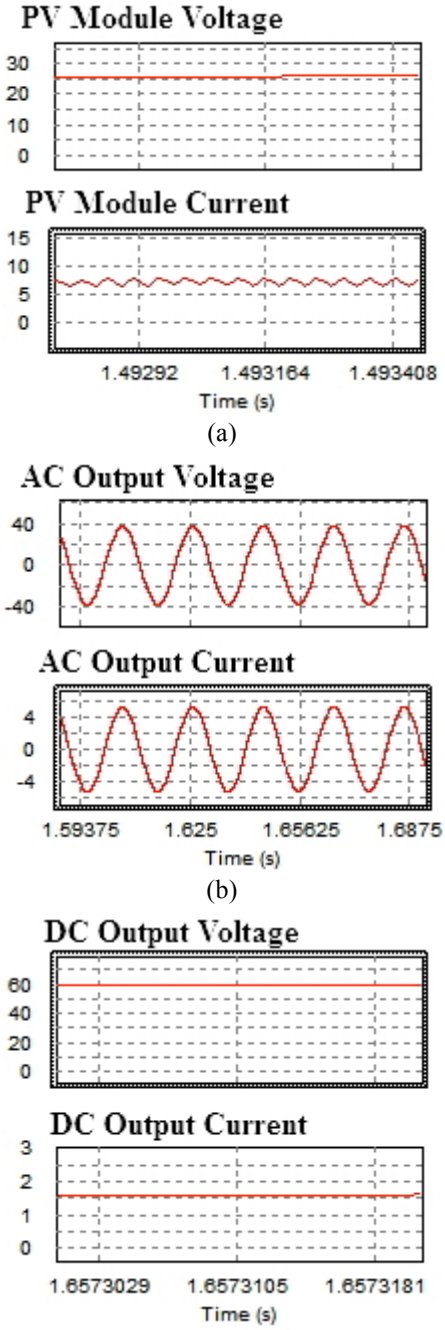

Fig. 13. Voltage and Current waveforms of (a) PV module (b) dc output and (c) ac output of QBDHC.

5. Hardware Investigation of the Proposed Multi Output Converter Based Smart Home System

Photograph of the hardware set up of the developed system is shown in Fig.14. Magna power programmable dc power supply was used as the PV source for hardware testing of the proposed prototype.

The controller is implemented using analog output module, NI-DAQ 9263, CompactDAQ Chassis, NIDAQ 9174 and software NI LabVIEW. NI LabVIEW is integrated with NI-DAQ 9263 through DAQ assistant.

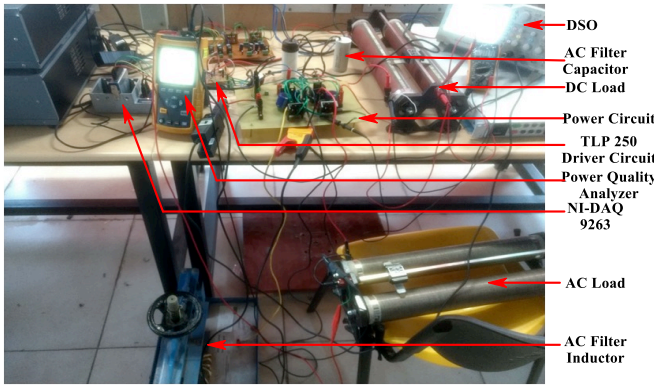

Fig. 14. Hardware setup photograph of the proposed system.

Figure 15, shows the controller developed in LabVIEW for generating the required gate pulses which are used to drive the hybrid converter switches.

The controller, as shown in Fig.7 is implemented in hardware and experimental waveforms of different signals are shown in Fig.16.

5.1 Experimental results of the proposed system using BDHC

Figure 17 shows the gate pulses, $V_{GS1} - V_{GS4}$. The waveforms of the PV module voltage, V_{pv} & PV module current, I_{pv} are shown in Fig.18 and it's values were found to be 24.5 V & 8.26 A respectively. Figure 19, shows the waveforms of dc output voltage, V_{dc} and current, I_{dc}. It was found that dc output voltage is 57.2 V and dc output current is 1.41 A. From the results, it is inferred that PV module voltage of 24.5 V is boosted to dc output voltage of 57.2 V. Figure 20a shows the waveforms of output ac voltage & current with filter, which depicts output ac voltage, V_{ac} of 17.07 V and output ac current, I_{ac} of 5.27 A respectively.

From Fig.20b, the output ac power was found to be 90 W at unity power factor. From the experimental results, it was found that, out of generated PV module power of approximately 202 W, 80 W is fed to the dc load and 90 W is fed to the ac load, contributing to overall system efficiency of 84 %.

THD of output ac voltage with filter is found to be 3.7 % as shown in Fig.21, which is within the permissible harmonic contents limit as per IEEE standard.

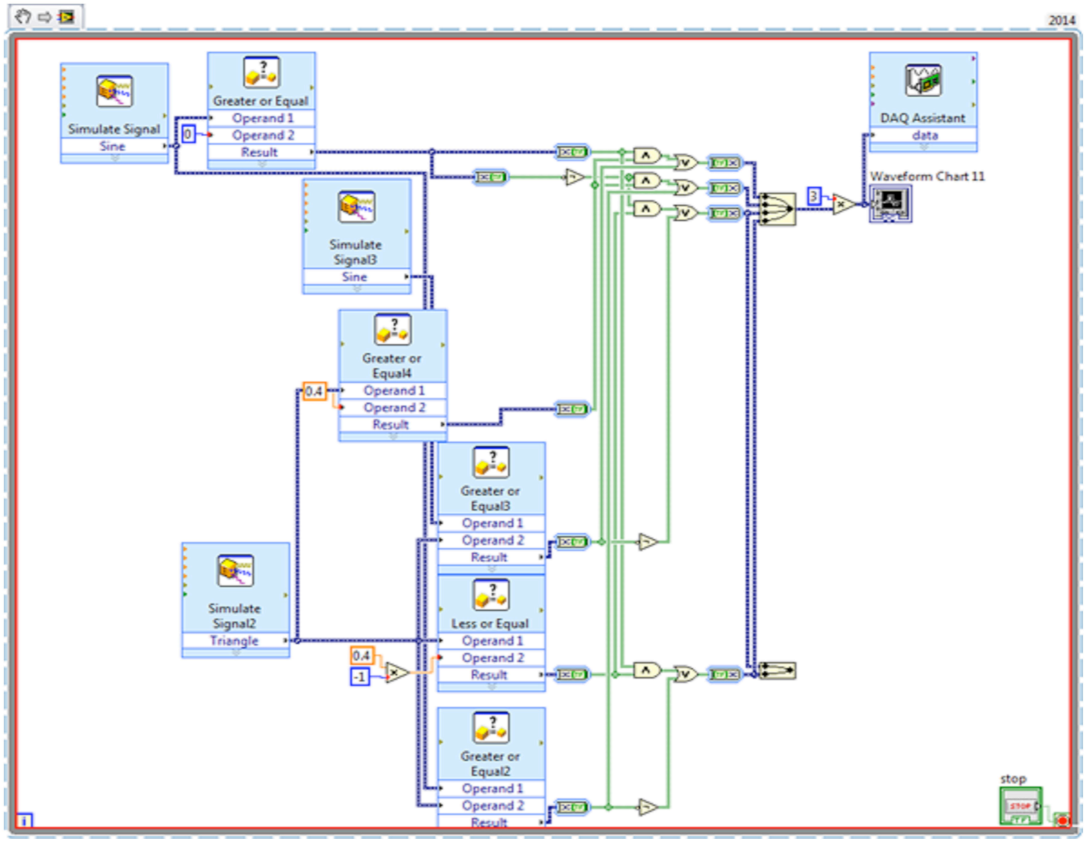

Fig. 15. Controller Model in LabVIEW.

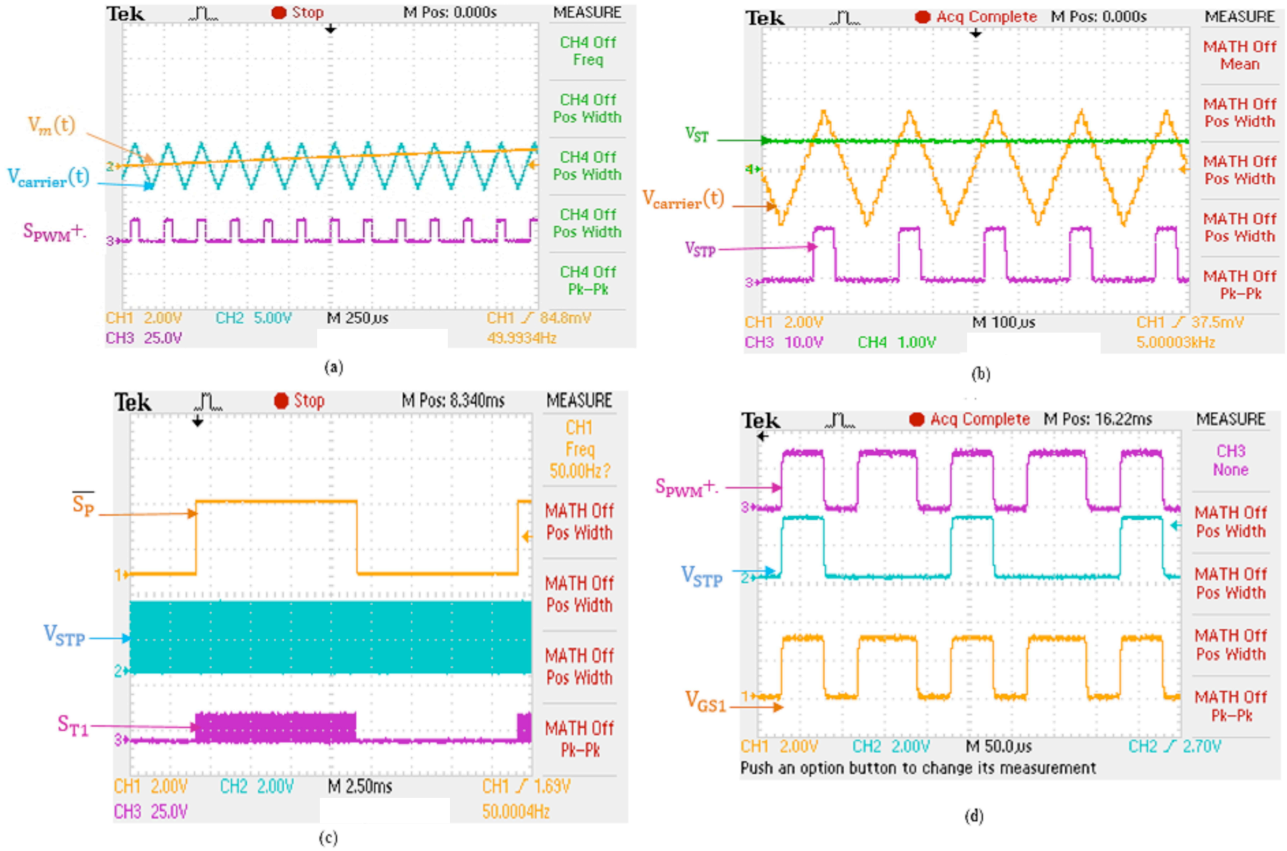

Fig. 16. Waveform of different stages of controller (a) Generation of SPWM, (b) Shoot-through pulse, V_{STP}, (c) S_{T1}, (d) Gate pulse, V_{GS1}.

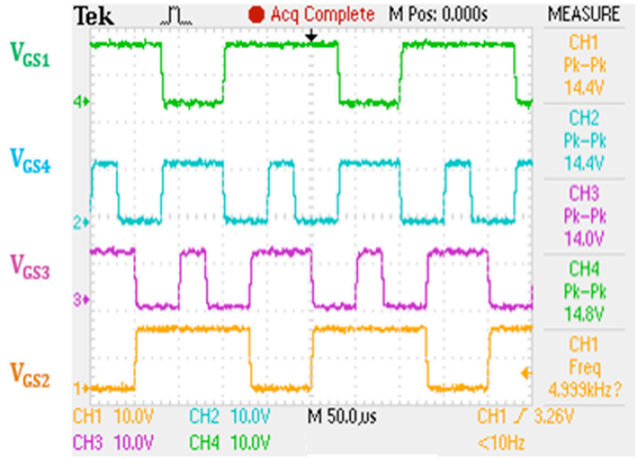

Fig. 17. Gate pulses for the converter switches.

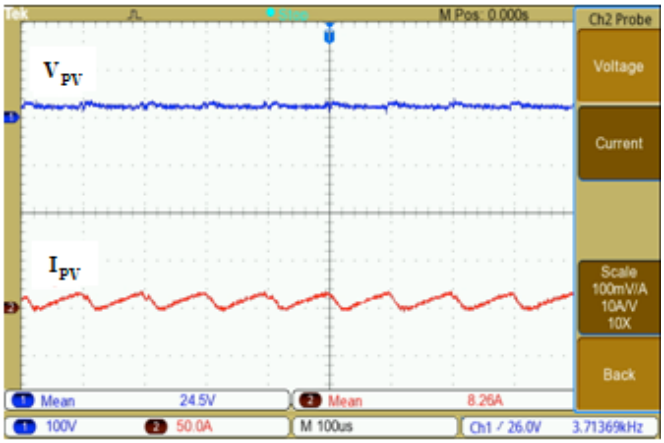

Fig. 18. Waveforms of PV module Voltage and Current of BDHC.

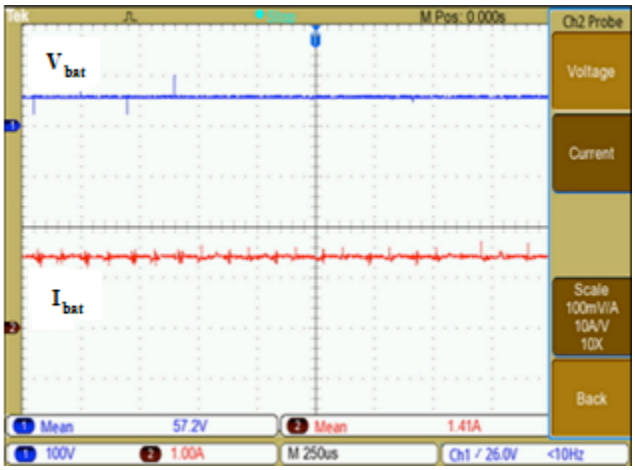

Fig. 19. Waveforms of dc output Voltage and Current of BDHC.

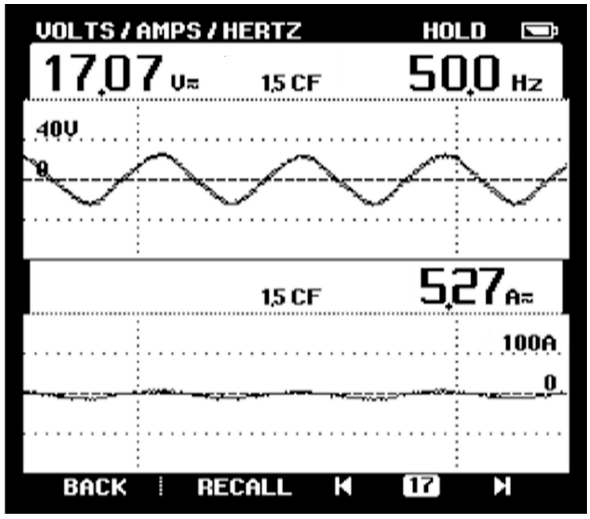

(a)

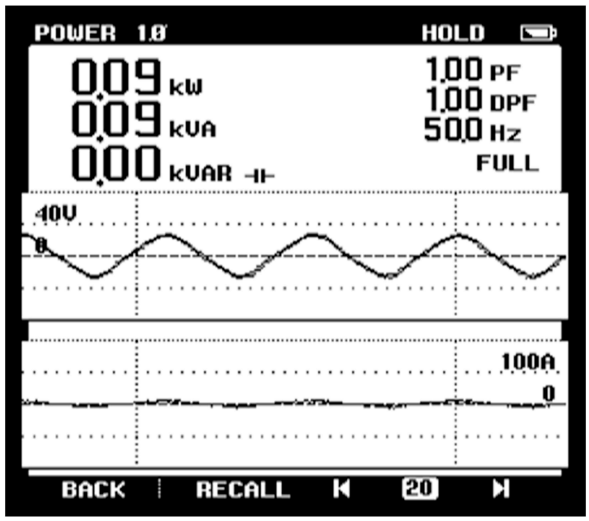

(b)

Fig. 20. Experimental results with BDHC (a) AC output voltage and current waveforms, (b) AC output power.

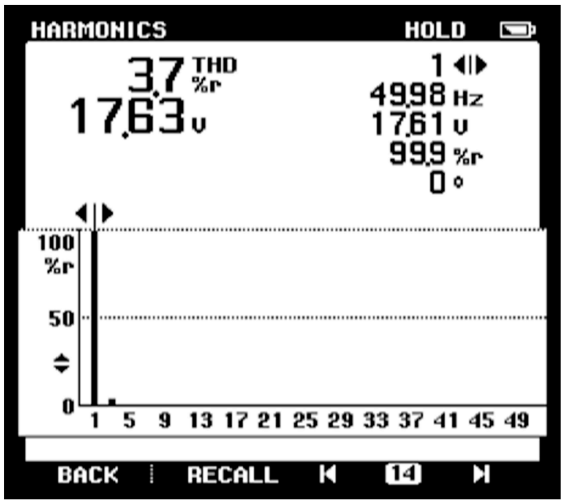

Fig. 21. THD of output AC voltage with Filter.

5.2 Experimental results of proposed multi output smart home system with QBDHC

Fig.22 shows the gate pulses $V_{GS1}-V_{GS4}$ with a shoot-through duty ratio of 0.36 and modulation index of 0.64. Figure 23a shows the PV module voltage, V_{pv} of 23.9 V and PV module current, I_{pv} of 8.3 A and Fig.23b shows the waveforms of dc output voltage, V_{dc} of 58.5 V & dc output current, I_{dc} of 1.45 A. From the experimental results it is inferred that, PV module voltage of 23.9 V is boosted to 58.5 V.

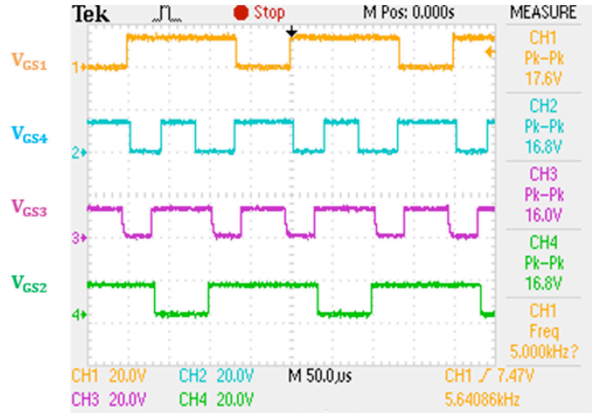

Fig. 22. Gate pulses for the converter switches.

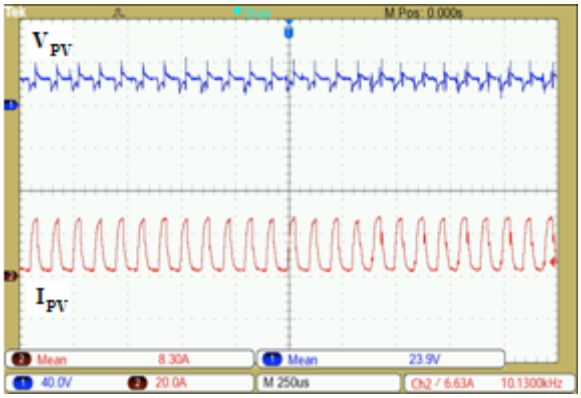

(a)

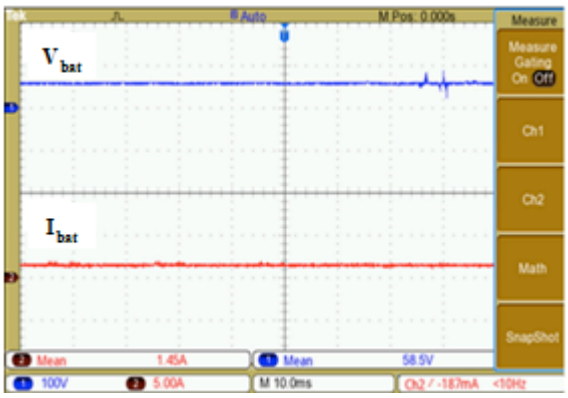

(b)

Fig. 23. Voltage and current waveforms across (a) PV module, (b) dc output.

Figure 24a shows the waveforms of ac load voltage and current with filter, which depicts output ac voltage, V_{ac} of 22.64 V and output ac current, I_{ac} of 3.79 A. From Fig.24b, the output ac power was found to be 86 W at unity power factor. From the experimental results, it was found that, out of the generated PV module power of approximately 198 W, 84 W is fed to the dc load and 86 W is fed to the ac load contributing to the overall system efficiency of 85 %. Figure 25 shows THD of output ac voltage with filter. It is observed that THD of output ac voltage with filter is obtained as 3.7 %, which is within the permissible THD limit as per the IEEE standard.

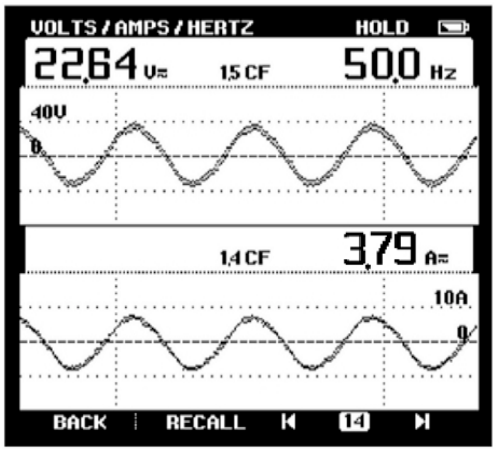

(a)

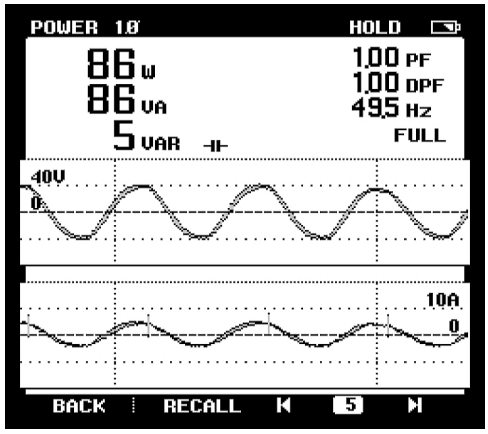

(b)

Fig. 24. Experimental results with QBDHC (a) AC output voltage and current waveforms, (b) AC output power.

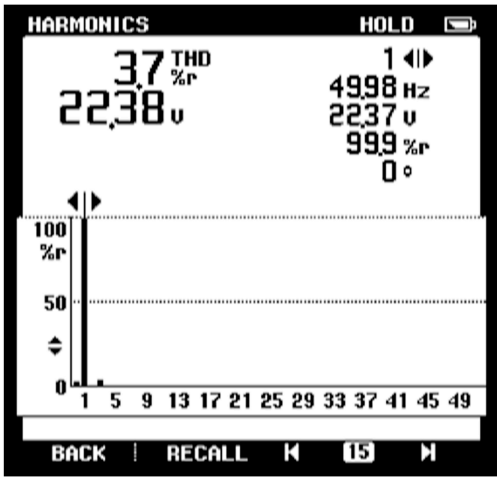

Fig. 25. THD of output ac Voltage with filter.

It can be observed from Section 4 and Section 5 that the experimental results harmonize with the simulation results validating the efficacy of the proposed multi output hybrid converter based modified smart home system.

6. Conclusion

This paper describes a novel system which integrates a rooftop PV module with smart home system by using multi output hybrid converter. The proposed prototype was designed for a 200 W system producing battery and ac power of 100 W at each output terminals. The system behavior is observed using PSIM simulation software and a hardware prototype was fabricated and tested for a 200 W system. For ideal lossless conditions, the overall system efficiency was observed as 98 % from simulation studies. The total harmonic distortion of the ac output voltage is found to be 3.7 % from the experimental investigations which is well within the IEEE standards. Similarity between the simulation results and experimental results validates the proposed system.

7. Reference

[1] A. S. Aziz, M. F. N. bin Tajuddin, and M. R. bin Adzman, "Feasibility Analysis of PV/Wind/Battery Hybrid Power Generation: A Case Study," Int. J. Renew. Energy Res., vol. 8, no. 2, pp. 661–671, 2018.

[2] O. Babacan, W. Torre, and J. Kleissl, "Siting and sizing of distributed energy storage to mitigate voltage impact by solar PV in distribution systems," Sol. Energy, vol. 146, pp. 199–208, Apr. 2017.

[3] S. Krithiga and N. Ammasai Gounden, "Investigations of an improved PV system topology using multilevel boost converter and line commutated inverter with solutions to grid issues," Simul. Model. Pract. Theory, vol. 42, pp. 147–159, 2014.

[4] K. Sundareswaran, K. A. Kumar, and P. R. Venkateswaran, "Dual input autonomous solar photovoltaic powered motor drive system for industrial applications," J. Renew. Sustain. Energy, vol. 7, no. 1, p. 013128-1-013128-13 Sundareswaran,, Jan. 2015.

[5] E. Scolari, F. Sossan, and M. Paolone, "Photovoltaic-Model-Based Solar Irradiance Estimators: Performance Comparison and Application to Maximum Power Forecasting," IEEE Trans. Sustain. Energy, vol. 9, no. 1, pp. 35–44, Jan. 2018.

[6] A. A. A. Radwan, Y. A.-R. I. Mohamed, and E. F. El-Saadany, "Assessment and performance evaluation of DC-side interactions of voltage-source inverters interfacing renewable energy systems," Sustain. Energy, Grids Networks, vol. 1, pp. 28–44, Mar. 2015.

[7] A. R. Bhatti, Z. Salam, M. J. B. A. Aziz, and K. P. Yee, "A critical review of electric vehicle charging using solar photovoltaic," Int. J. Energy Res., vol. 40, no. 4, pp. 439–461, Mar. 2016.

[8] C. Balaji, S. S. Dash, N. Hari, and P. C. Babu, "A four port non-isolated multi input single output DC-DC converter fed induction motor," in 2017 IEEE 6th International Conference on Renewable Energy Research and Applications (ICRERA), 2017, January, pp. 631–637.

[9] O. Ray and S. Mishra, "Boost-Derived Hybrid Converter With Simultaneous DC and AC Outputs," IEEE Trans. Ind. Appl., vol. 50, no. 2, pp. 1082–1093, Mar. 2014.

[10] P. Patra, A. Patra, and N. Misra, "A Single-Inductor Multiple-Output Switcher With Simultaneous Buck, Boost, and Inverted Outputs," IEEE Trans. Power Electron., vol. 27, no. 4, pp. 1936–1951, Apr. 2012.

[11] T. Mori, H. Funato, S. Ogasawara, F. Okazaki, and Y. Hirota, "H-bridge step-down converter applied proposed switching transient waveform modification to reduce specific harmonics," in 2012 International Conference on Renewable Energy Research and Applications (ICRERA), 2012, pp. 1–6.

[12] M. Unlu, S. Camur, E. Beser, and B. Arifoglu, "A Current-Forced Line-Commutated Inverter for Single-Phase Grid-Connected Photovoltaic Generation Systems," Adv. Electr. Comput. Eng., vol. 15, no. 2, pp. 85–92, 2015.

[13] N. A. Samsudin, D. Ishak, and A. B. Ahmad, "Design and experimental evaluation of a single-stage AC/DC converter with PFC and hybrid full-bridge rectifier," Eng. Sci. Technol. an Int. J., vol. 21, no. 2, pp. 189–200, Apr. 2018.

[14] S. Inoue and H. Akagi, "A bidirectional isolated dc-dc converter as a core circuit of the next-generation medium-voltage power conversion system," IEEE Trans. Power Electron., vol. 22, no. 2, pp. 535–542, 2007.

[15] A. Ahmad, V. K. Bussa, R. K. Singh, and R. Mahanty, "Quadratic boost derived hybrid multi-output converter," IET Power Electron., vol. 10, no. 15, pp. 2042–2054, Dec. 2017.

[16] R. Adda, S. Mishra, and A. Joshi, "A PWM control strategy for switched boost inverter," in 2011 IEEE Energy Conversion Congress and Exposition, 2011, pp. 991–996.

[17] M. H. Shwehdi and S. R. Mohamed, "Proposed smart DC nano-grid for green buildings- A reflective view," in 2014 International Conference on Renewable Energy Research and Application (ICRERA), 2014, pp. 765–769.

[18] D. P. Andrea, D. N. L. Pio, and M. Santolo, "Super twisting sliding mode control of smart-inverters grid-connected for PV applications," in 2017 IEEE 6th International Conference on Renewable Energy Research and Applications (ICRERA), 2017, January, pp. 793–796.

[19] Y. Fayyad and L. Ben-Brahim, "Multilevel cascaded Z source inverter for PV power generation system," in 2012 International Conference on Renewable Energy Research and Applications (ICRERA), 2012, pp. 1–6.

[20] S. Krithiga, D. R. B. B. Jose, H. R. Upadhya, and N. A. Gounden, "Grid-Tied Photovoltaic Array Using Power Electronic Converters with Fuzzy Logic Controller for Maximum Power Point Tracking," Aust. J. Electr. Electron. Eng., vol. 9, no. 4, pp. 393–400, Jan. 2012.

[21] F. Sossan and M. Paolone, "Integration and Operation of Utility-Scale Battery Energy Storage Systems: the EPFL's Experience," IFAC-Papers On Line, vol. 49, no. 27, pp. 433–438, 2016.

[22] S. Jeyasudha and B. Geethalakshmi, "Modeling and Analysis of a Novel Boost Derived Multilevel Hybrid Converter," Energy Procedia, vol. 117, pp. 19–26, 2017.

[23] B. Bilgin and A. Emadi, "Electric Motors in Electrified Transportation: A step toward achieving a sustainable and highly efficient transportation system," IEEE Power Electron. Mag., vol. 1, no. 2, pp. 10–17, Jun. 2014.

[24] T. H. Ortmeyer and P. Pillay, "Trends in transportation sector technology energy use and greenhouse gas emissions," Proc. IEEE, vol. 89, no. 12, pp. 1837–1847, 2001.

[25] K. Jyotheeswara Reddy and S. Natarajan, "Energy sources and multi-input DC-DC converters used in hybrid electric vehicle applications – A review," Int. J. Hydrogen Energy, vol. 43, no. 36, pp. 17387–17408, 2018.

[26] M. Yilmaz and P. T. Krein, "Review of Battery Charger Topologies, Charging Power Levels, and Infrastructure for Plug-In Electric and Hybrid Vehicles," IEEE Trans. Power Electron., vol. 28, no. 5, pp. 2151–2169, May 2013.

[27] P.-Y. Kong and G. K. Karagiannidis, "Charging Schemes for Plug-In Hybrid Electric Vehicles in Smart Grid: A Survey," IEEE Access, vol. 4, no. 99, pp. 6846–6875, 2016.

[28] C. Capasso, S. Riviera, S. Kouro, and O. Veneri, "Charging Architectures Integrated with Distributed Energy Resources for Sustainable Mobility," Energy Procedia, vol. 105, pp. 2317–2322, May 2017.

[29] J. Y. Yong, S. M. Fazeli, V. K. Ramachandaramurthy, and K. M. Tan, "Design and development of a three-phase off-board electric vehicle charger prototype for power grid voltage regulation," Energy, vol. 133, pp. 128–141, Aug. 2017.

[30] T. M. Blooming and D. J. Carnovale, "Application of IEEE STD 519-1992 Harmonic Limits," in Conference Record of 2006 Annual Pulp and Paper Industry Technical Conference, 1992, pp. 1–9.

[31] S. Krithiga and N. Ammasai Gounden, "An Improved Power Electronic Controller with Unity Power Factor for a Single-Stage Grid-Tied PV System," Arab. J. Sci. Eng., vol. 39, no. 10, pp. 7173–7182, Oct. 2014.